GALILEAN ELECTRODYNAMICS

Contents

Mailing Address:
Galilean Electrodynamics
141 Rhinecliff Street
Arlington, MA 02476-7331, U.S.A.

The New Fundamental Trajectories: Part 1 - Hyperbolic/Elliptic Trajectories

Joseph J Smulsky
Institute of Earth's Cryosphere
Siberian Branch of Russian Academy of Sciences
P O Box 1230, Tyumen, 625000, RUSSIA, e mails smulski@ikz.ru, jsmulsky@mail ru

Fundamental trajectories are predicted from the interaction of two charged bodies We use classical mechanics, *i e*, mass is constant and force depends on relative distance and velocity The possible range of trajectories is analyzed At small velocities the trajectories are classical, and at large velocities they become relativistic Forces arising from new mechanisms can explain both microcosm and macrocosm Part 1 considers hyperbolic trajectories

Key words: force, motion, trajectories, kinematics, momentum pericenter, apocenter, attraction, repulsion

1. Introduction

Modern atomic physics focuses on random events described by statistical probabilistic principles For example, according to Heisenberg's point-of-view one cannot know the exact position and velocity of a particle in orbit, but one can still describe these attributes with some probability In an atom, the microcosm can be described with the assistance of probabilistic functions, but not by trajectories taken by particles

Limitations on the precision of measurements on a moving particle make absolute knowledge of a particle's position and momentum impossible, but do not mean that a particle's position and momentum do not *exist* in theory and reality Therefore scientists now and again return to the problem of determined motions This was clearly evident in the public discussion which was organized by the Editors of Apeiron (see Apeiron, 1995, vol 2, no 4) The present paper considers the interactions of two charged particles, accurately predicts some fundamental trajectories, and examines their characteristics

Interaction of two charged bodies depends on not only the distance but also the velocity between them According to the Theory of Relativity (TR), the mass-velocity relation expresses the dependence of the interaction upon velocity However, the authors of paper [1] have shown that the *mass* of a body should be constant, but the *force* on it should depend on velocity $\mathbf{F} = \mathbf{F}_0 f(v/c)$, where $\mathbf{F}_0$ is the force of interaction between two bodies when they are in relative rest, *i e* their relative velocity $\mathbf{v} = 0$, $f(v/c)$ is the *effectiveness coefficient*, which is a function of v/c, where c is the velocity of the transmitted interaction.

Other investigators have proposed expressions for interaction forces which depend not only on distance and velocity, but also on *acceleration* [2,3] In our opinion, any dependence of the force $\mathbf{F}$ on acceleration has a shortcoming: it is expressed *non explicitly*, since according to the Newton's second law $\mathbf{F} = m\mathbf{a}$, the summands with acceleration $\mathbf{a}$ should be on the right-hand side of this equality but not on the left-hand side There are many contradictions in a force law involving acceleration We do not focus on them here, as this kind of 'force law' contradicts the essence of 'force'

If one body acts on another, then the result is an acceleration of the second body In other words, the acceleration is an expression of this effect From another point of view, one measures the effect by the assistance of a force For the purpose of measuring an effect (of acceleration) on a second body, one detects the motions of the second body by assistance of a third body—for example, a spring and its deformation—in order to define the force magnitude Therefore, both *force* and *acceleration* define the action on the body They are the same phenomenon Acceleration exists objectively, but Newton has introduced the concept of force to describe the measurable effect

The proportionality coefficient (m) between the force and the acceleration is due to a choice of standards (for example, the platinum-iridium cylinder with height and diameter of 39 mm, which we call one kilogram) By this standard, we establish measurement units for acceleration and force Thus, Newton's second law $\mathbf{F} = m\mathbf{a}$ is expressing the relationship of force and acceleration [4]

So, if we set forth a force, then acceleration is specified By assistance of *integration*, we find speed $v(t)$, and position $S(t)$, *i e* we find all parameters of a body's motion So, the *force* cannot depend on acceleration, but it can depend on velocity and distance—which are relative to the causative body

2. Interaction Depending on Distance and Velocity

Our investigations [5,6] have shown that the force of one point-charge q_1 acting on another charge q_2 moving with velocity $\mathbf{v}$ through separation $\mathbf{R}$ is

$$\mathbf{F} = \frac{q_1 q_2}{\varepsilon}\mathbf{R}(1-\beta^2)\Big/\left[R^2 - |\bar{\beta}\times\mathbf{R}|^2\right]^{3/2} \qquad (1)$$

where $\bar{\beta} = \mathbf{v}/c_1$, $c_1 = c/\sqrt{\varepsilon\mu}$, c is the speed of light in vacuum, ε and μ are the dielectric and magnetic permeability of the medium in which the charged objects are located It should be noted that similar results were obtained by other researchers [7]

The force (1) can be written in a form $\mathbf{F} = \mathbf{F}_0 f(\beta)$ where

$$\mathbf{F}_0 = \frac{q_1 q_2 \mathbf{R}}{\varepsilon R^3} \text{ and } f(\beta) = (1-\beta^2)\Big/\left[1-|\bar{\beta}\times\mathbf{R}/R|^2\right]^{3/2}$$

When charge velocity **v** is small, the force (1) coincides with Coulomb's law. But as the velocity increases, the force decreases to zero (except for $\bar{\beta}$ exactly perpendicular to **R**). That is, we let the charge speed approach the maximum limit on the speed of electromagnetic propagation ($\beta \to 1$), and at this limit, no action is exerted on the charged body, and it is not accelerated.

According to (1) and the second law of Newton, the acceleration of one charge relative to another will be written as

$$\frac{\mathbf{d}^2\mathbf{R}}{\mathbf{d}t^2} = \mu_1 \mathbf{R}(1-\beta^2)\Big/\left[R^2-|\bar{\beta}\times\mathbf{R}|^2\right]^{3/2} \qquad (2)$$

where μ_1 is the interaction constant.

$$\mu_1 = q_1 q_2 (m_1 + m_2)/\varepsilon\, m_1 m_2 \qquad (3)$$

As a result of solving Eq. (2) [8], we obtained a trajectory in a polar coordinate system as follows:

$$\varphi = \int (R^2 v_r)^{-1} dR \qquad (4)$$

where

$$v_r = c_1 \sqrt{1 - \frac{h^2}{c_1^2 R^2} - \left[1 - \frac{v_{r0}^2}{c_1^2} - \frac{h^2}{c_1^2 R_0^2}\right]\exp[f(...)]} \qquad (5)$$

with

$$f(...) = \frac{2\mu_1}{c_1^2}\left(1\Big/\sqrt{R^2 - h^2/c_1^2} - 1\Big/\sqrt{R_0^2 - h^2/c_1^2}\right)$$

where v_r is the radial velocity, v_{t0} and v_{r0} are the transverse and radial components of velocity on the radius R_0, and $h = v_{t0}R_0 = v_t R$ is the kinematic momentum, which is constant for all points of the trajectory.

3. Some Interaction Limits

Equations (1) to (5) describe interactions propagating with the final velocity c_1. If, as in General Relativity Theory (GRT), the gravitational action is considered to propagate with light velocity c_1, then these expressions will also describe gravity. In this case the interaction constant is

$$\mu_1 = -G(m_1 + m_2) \qquad (6)$$

Equations in GRT are solved approximately by expansion in a series and retaining all terms up to second order in β. If we expand the series with respect to c_1^2 with in the same accuracy, and substitute Eq. (5) into (4), then we obtain the equation of motion in a centrally symmetric field in GRT [9]

$$\varphi = \int \left[R^2\sqrt{c_1^2 + v_0^2 - (c_1^2 + h^2/R^2)(1 - R_g/R)}\right]^{-1} h\, dR \qquad (7)$$

where $R_g = -2\mu/c_1^2$ is called a gravitational radius.

Consider the limiting case of small velocities. First we shall reduce Eqs. (4) and (5) to the relative form

$$\varphi = \int (\bar{R}^2 \bar{v}_r)^{-1} d\bar{R} \qquad (8)$$

with

$$\bar{v}_r = \frac{1}{\beta_p}\sqrt{1 - \frac{\beta_p^2}{\bar{R}^2} - \left(1-\beta_p^2\right)\exp[f(...)]} \qquad (9)$$

where

$$f(...) = 2\alpha_1\beta_p^2\left(1\Big/\sqrt{\bar{R}^2 - \beta_p^2} - 1\Big/\sqrt{1-\beta_p^2}\right)$$

Here $\bar{R} = R/R_p$ is the relative radius; R_p is the radius to the nearest point of the trajectory (pericenter), at which also $v_{R0} = 0$; $\bar{v}_r = v_r/v_p$ is the relative radial velocity; v_p is the tangential velocity at the pericenter; $\beta_p = v_p/c_1$; and $\alpha_1 = \mu_1/(R_p v_p)^2$ is the trajectory parameter. It has been shown in [8] that when $c_1 \to \infty$, Eq. (5) passes to the classical expression

$$v_r = \sqrt{v_{r0}^2 + \left(\mu_1/h + h/R_0\right)^2 - \left(\mu_1/ + h/R\right)^2} \qquad (10)$$

After referring v to the parameters at the pericenter, the relative radial velocity is

$$\bar{v}_r = \sqrt{(\alpha_1+1)^2 - (\alpha_1 + 1/\bar{R})^2}$$

Integrating (8) with the boundary conditions $\varphi = 0$ and $\bar{R} = 1$, we get the equation of fundamental classical trajectories:

$$\bar{R} = 1/[(\alpha_1 + 1)\cos\varphi - \alpha_1] \qquad (11)$$

The form of trajectories is defined by the value of the parameter α_1 as follows: Circle: $\alpha_1 = -1$; Ellipse: $-1 < \alpha_1 < -0.5$; Parabola: $\alpha_1 = -0.5$; Hyperbola: $-0.5 < \alpha_1 < 0$; Straight Line: $\alpha_1 = 0$. Thus Eqs. (4), (5), (8) and (9) represent the most common fundamental trajectories, which are valid both for small velocities of motion and large velocities tending to the speed of light. In contrast to classical trajectories, these trajectories are biparametric; they depend not only on α_1 but also the relative velocity β_p. Therefore, they are of both physical and mathematical interest.

4. Numerical Method, Asymptotic Solution and Hyperbolic Trajectories

Equation (8) was integrated numerically using a PC AT computer with the help of the MathCAD program To increase the speed and accuracy of integration, the region of changing relative radius $\bar{R}$ was divided into domains, integration was performed in each domain, and then the results were combined Using asymptotic solutions given in the Appendix and test samples, we found that the integration error does not exceed one part per thousand The parameters were varied in computations as indicated $\alpha_1 = (-0.1; -0\,2; -0.3, -0.4; -0.5; -0.6; -0.7; 0.8; -0.9)$ and $\beta_p = (0.1; 0\,3; 0.7; 0\,9)$

The values of other parameters, which were defined by the peculiarities of trajectories, are also given The computer programs were written in FORTRAN Only the most characteristic types of trajectories are presented below

One-sided branches of the hyperbolic trajectories are shown in Fig 1 in a Cartesian system of coordinates ($\bar{x} = x/R_p$ and $\bar{y} = y/R_p$) The attracting center is at the origin of the coordinate system, and a particle moves from the pericenter at $\bar{x} = 1$; $\bar{y} = 0$ to a location at infinity or *vice versa* A smooth and continuous process of integration is possible for all trajectories except No 7.

When $\beta_p = 0.1$, the trajectory virtually coincides with the classical one. With an increase in velocity at the pericenter, the angle between asymptotes φ_a decreases With velocity limit β_p equal to β_{pc} with the value 0 954, the angle between asymptotes becomes negative

Trajectory 7 differs from the others not only by the angle $\varphi_a < 0$ To this end, let us consider some details of the integration. The point $\bar{R} = 1$ is a singular point of integral (8) since it converts (9) to zero Therefore the numerical integration was performed from $\bar{R} = 1\,001$ to $\bar{R} = 1000$, and the angle increment φ in the region $1 < \bar{R} < 1\,001$ is the asymptotic solution

$$\varphi = \sqrt{\bar{R}^2 - 1} \Big/ \bar{R}\sqrt{1 + \alpha_1 \Big/ \sqrt{1 - \beta_p^2}} \qquad (12)$$

the derivation of which is given in the Appendix As one can see, the denominator in the first multiplier vanishes with

$$\beta_p = \beta_{pc} = \sqrt{1 - \alpha_1^2} \qquad (13)$$

In this case when $\beta_{pc} = 0\,954$ and $\bar{R}$ approaches 1, the angle φ tends to infinity. This result was verified by numerical integration, namely, by sequential setting of the integration variable starting at $\bar{R} = 1\,0001$ and then increasing slightly to $\bar{R} = 1\,00001$, *etc* Thus the particle on the trajectory with limiting velocity β_{pc} at the pericenter, while moving from infinity, reaches a circle with radius $\bar{R} = 1$ and rests on it infinitely long—i e , the particle moving from infinity is captured by the attracting center into a circular orbit

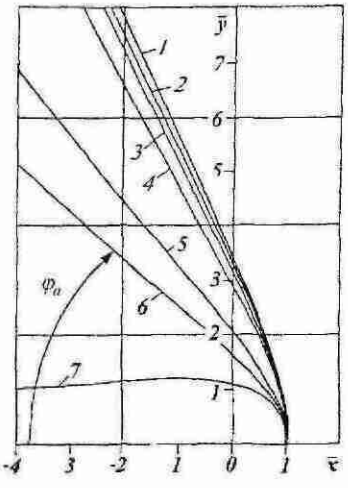

Figure 1 The trajectory at $\alpha_1 = -0\,3$ and sub-light speed at the pericenter ($\beta_p \le \beta_{pc}$) with half-angles between asymptotes φ_a, and approaching velocities $\beta_{r\infty}$ as $R \to \infty$ infinity (Integration begins at $\bar{R} = 1.001$ for trajectory 7).

№	1	2	3	4	5	6	7
β_p	0 1	0 3	0 5	0 7	0 9	0 93	0 954
α	- 006	-0 054	-0 15	-0 294	-0 486	-0 519	-0 546
$\beta_{r\infty}$	0 063	0 208	0 329	0 480	0 649	0 668	0 667
φ_a^0	64 8	64 4	63 8	61 9	50 6	40 3	-5 58'

We consider this process in more detail With φ approaching infinity, a circular orbit is feasible at $\bar{v}_r = 0$ in Eq. (8) Then from Eq (9), with allowance for this condition when $\bar{r} \to \infty$, we get

$$\alpha_1 = \frac{0.5\ln\left[(1 - \beta_p^2/\bar{R}^2)/(1 - \beta_p^2)\right]}{\beta_p^2/\sqrt{\bar{R}^2 - \beta_p^2} - \beta_p^2\Big/\sqrt{\bar{R}^2 - \beta_p^2}} \qquad (14)$$

The radius of a circular orbit is simultaneously that of the pericenter, i e $\bar{R} = 1$. Having found the limit of the right-hand side (14) where $\alpha_{1c} = \alpha_1$ and $\beta_{pc} = \beta_p$ for a circular orbit, we get

$$\alpha_{1c} = -\sqrt{1 - \beta_{pc}^2} \qquad (15)$$

With small velocities ($\beta_p \to 0$), it follows from (15) that $\alpha_1 = -1$ This corresponds to a circular orbit Since Eqs (13) and (15) are identical, this fact convinces us again that trajectory 7, having attained the limiting velocity β_{pc} at the pericenter, passes to a circular orbit as shown in Fig 1

Figure 1 also shows the radial velocities of particles at maximum velocity $\beta_{r\infty}$ and half-angle φ_a between asymptotes For trajectory 7, the plotting begins at $\overline{R} = 1.001$ Usually, with an increase in the velocity of the particle as $R \to \infty$, its velocity also increases at the pericenter The violation of this rule for trajectories 6 and 7 is accounted for by the fact that the trajectory parameter α_1 depends on velocity at the pericenter v_p Therefore it is expedient to consider the interaction parameter α, which is independent of velocity

$$\alpha = 2\mu_1 / R_p c_1^2 = -R_g / R_p \qquad (16)$$

and related to α_1 as

$$\alpha = 2\alpha_1 \beta_p^2 \qquad (17)$$

As is seen from Fig 1, the modulus of the interaction parameter α_1 for all hyperbolic trajectories is less that 1, *i e* according to (16) the pericenter radius is larger than the gravitational one

The *limited range* is the third property of trajectory 7 in Figure 1 In the region $\beta_{pc} < \beta_p < 1$ the radicand in (9) is negative, *i e* no trajectories exist In order to numerically study the other possible trajectories, the parameters of Eqs (4) and (5) were referred to parameters v_{t0}, R_0 at an arbitrary point of the trajectory In this case, Eq (8) remains without change, and instead of (9) we get

$$\overset{-0}{v}_r = \frac{1}{\beta_{t0}} \sqrt{1 - \beta_{t0}^2 / \overline{R}^2 - \left(1 - \beta_{r0}^2 - \beta_{t0}^2\right) \exp f(...)} \qquad (18)$$

with

$$f(...) = 2\alpha_1^0 \beta_{t0}^2 \left(1/\sqrt{\overline{R}^2 - \beta_{t0}^2} - 1/\sqrt{1 - \beta_{t0}^2} \right)$$

where

$$\overline{R} = \frac{R}{R_0}, \quad \beta_{t0} = \frac{v_{t0}}{c_1}, \quad \overset{-0}{v}_r = \frac{v_r}{v_{t0}}, \quad \beta_{r0} = \frac{v_{r0}}{c_1}, \quad \alpha_0^1 = \frac{\mu_1}{R_0 v_{t0}^2}$$

Equations (8) and (18) were integrated in two regions, $\overline{R} > 1$ and $\overline{R} < 1$ Values of $\beta_{t0} > \beta_{pc}$ were given to the relative transverse velocity, and the radial velocity β_{r0} was varied (see Fig 2) In all calculations, we found that a decrease in $\overline{R}$ to a certain value $\overline{R} \to \beta_0$ made the radial velocity tend to zero, *i e*, this point is the pericenter $\overline{R} = R_p$ And the value $R_p / R_0 = \beta_{t0} = 1$ indicates according to the momentum conservation law $\overline{h} = \overline{R}\beta_{t0} = 1$ that the transverse velocity at this point tends to the speed of light but does not reach it, *i e* $\beta_p = \beta_{p0} = v_p / c_1 = 1_{-0}$ These trajectories with almost light speed at the pericenter are renormalized to R_p and presented in Fig 2 Since the trajectory parameter $\alpha_1 = \mu_1 / h v_p$ is related to $\alpha_1^0 = \mu_1 / h v_{t0}$ as

$$\alpha_1 = \alpha_1^0 \beta_{t0} \qquad (19)$$

it follows that in this case $\alpha_1 \approx -0.3$, and trajectories of Fig 2 may be considered as continuation of trajectories of Fig 1 with the particle velocity increasing to infinity However, in contrast to the trajectories of Fig 1, with an increase in $\beta_{r\infty}$ (see, trajectories 6, 5, 4, 3 and 2 of Fig 1), the angle φ_a between asymptotes increases For a particle moving with light speed ($\beta_{r\infty} = 1$), the angle is equal to $\pi/2$ (see trajectories with number 1), *i e* the particle with light speed moves along a vertical line

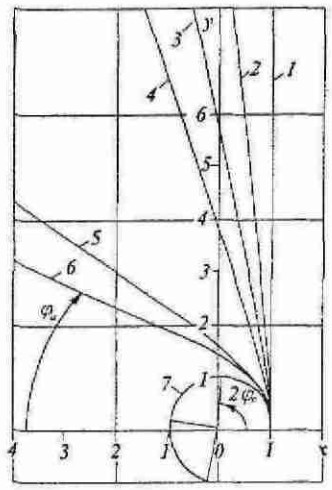

Figure 2 The trajectories at $\alpha_1^0 = -0.3$ and light speed at the pericenter ($\beta_p = 1_{-0}$)

N°	5	4	2	1	5	3	1	6	1	7	1
β_{t0}	0.96	0.96	0.96	0.96	0.97	0.97	0.97	0.98	0.98	0.987	0.987
α	-0.576	-0.576	-0.576	-0.576	-0.582	-0.582	-0.582	-0.588	-0.588	-0.592	-0.592
β_{r0}	0.1	0.2	0.25	0.28	0.1	0.2	0.243	0.1	0.199	0.1	0.161
$\beta_r^0 / \overline{R}_a^*$	0.712	0.850	0.949	1.0	707	897	1	0.681	1	1.04*	1
φ_a^0	35	73	84	90	35	78	90	23	90	41.2	90

Symbol * indicates data agreement

Numerical solutions have shown that trajectories with light speed at the pericenter are obtained at transverse particle velocity

$$\beta_{t0} > \beta_{pc} \tag{20}$$

However, with further increase in transverse velocity (see trajectory 7 in Fig 2) the orbit becomes ellipse like, and the angle of its apocenter from the pericenter is $\varphi_a = 41.2°$ In this case the period of return to the pericenter will be realized over an angle 82.4° and more than four such periods exist for one turn Since the radius of the apocenter $R_a = 1.04$ differs slightly from the pericenter radius, the motion will take places along the circular orbit with four small jumps per turn During jumps the particle velocity decreases, and then it tends to light speed at the pericenter Since in this case φ_a is not a multiple of π/n, where n is an integer, the location of pericenters will change The pericenters will rotate with an angle per turn of

$$\Delta\varphi_p = 2\varphi_a(n+1) - 2\pi \tag{21}$$

where n = INTEGER (π/φ_a) is an integer Apparently, for the ellipse-like orbits such as trajectory 7 of Fig 2, the radicand in (18) at large $\overline{R}$ should be negative We shall find the limiting parameters, α_{1p}^0, and $\beta_{0p} = \sqrt{\beta_{r0}^2 + \beta_{tp}^2}$, from the condition $\overline{v}_r^0 = 0$ $\overline{r}_r^0 = 0$ when $\overline{R} \to \infty$ After transformation of (18) we get

$$\alpha_{1p}^0 = \frac{1}{2}\beta_{tp}^{-2}\left[\sqrt{1-\beta_{tp}^2}\,\ln\left(1-\beta_{0p}^2\right)\right] \tag{22}$$

With $R_0 = R_p$ and small velocities when $\beta_{0p} = \beta_{tp} \to 0$, it follows that $\alpha_{1p}^0 = -0.5$, *i.e*, relation (22) determines the parameters of parabolic trajectories If the transverse velocity of the particle is larger than the limiting velocity β_{pc} and larger than β_{tp}, then the trajectory will be ellipse-like, and the particle will move at light speed at the pericenter

The parameters which produced the ellipse-like trajectories (Fig 3) were determined under the following conditions With an increase in the radial velocity for trajectories 1, 2 and 3, the excursion $\Delta\overline{R} = \overline{R}_a - 1$ and the angle of the apocenter increase With an additional increase in β_{p0} the value R_a grows continuously and the angle φ_a attains a maximum for trajectory 4 and then decreases In this case, trajectories 4 and 5 have apocenters which are away from the pericenters by more than one turn With a further increase in radial velocity, the trajectory (see line 5) is broken When β_0 approaches unity, trajectories are flattened (analogous to trajectories 1-3 in Fig 2), and at light speed they turn into straight lines The hyperbolic trajectories in Figures 1 and 2 may coincide in separate regions However, different interaction parameters correspond to the trajectories, and the velocities of the particle motion along them are different

Thus, in the region $-0.5 < \alpha_1 < 0$, particles have trajectories depending upon their velocities $\beta_p < \beta_{pc}$ produces hyperbolic-like trajectories, and $\beta_p = \beta_{pc}$ produces circular trajectories of particles captured as they arrive from great distances, or $\beta_{t0} > \beta_{pc}$ produces trajectories of particles moving at the speed of light In the last case, where $\beta_{t0} > \beta_{tp}$, the particle's orbit is ellipse-like, and the period of orbit can differ from 2π radians

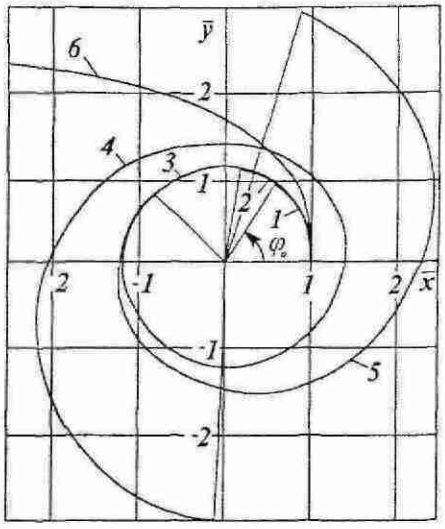

Figure 3 Ellipse-like trajectories (1-5) with light speed at the pericenter, $\beta_p = 1_{-0}$, $\alpha_1^0 = -0.498$, $\beta_{r\infty} = 0.93$, $\alpha = -0.926$

N°	1	2	3	4	5	6
β_{r0}	0.100	0.120	0.128	0.129	0.130	0.200
$\overline{R}_a / \beta_{r\infty}$	1.103	1.133	1.176	2.981	3.035	095*
φ_a^0	59.8	82.1	135.6	626.8	432.9	-18.24

Symbol * indicates data agreement

5. Conclusion

The calculated trajectories are based on force law (1) which was derived from the empirically established laws of electrodynamics The numerical solutions were derived on the basis of fundamental physics, logic and mathematics grounded in the scientific method The results agree with observed phenomena Therefore, two particles interacting under electrical forces will move along the trajectories presented in this paper If gravitational interactions are propagated with the speed of light, then two interacting point masses will move along these trajectories

6. Acknowledgment.

David L Bergman volunteered to help with the editing necessary for publishing my paper in English I am most grateful for his assistance

Appendix: Asymptotic Solutions

1. Solutions in the Vicinity of $\overline{R} = 1$

The radicand in (9) will be denoted by $f(\overline{R}^2)$ We shall expand $f(\overline{R}^2)$ in the vicinity of $\overline{R}^2 = 1$ with a Taylor series

$$f(\overline{R}^2) \approx f(1) + f'(1)(\overline{R}^2 - 1) + \frac{f''(1)}{2}(\overline{R}^2 - 1)^2 + \ldots \tag{1a}$$

Owing to the small difference between $\overline{R}^2$ and 1, we shall limit ourselves to terms of second order. According to (9) the derivative is of the form

$$\frac{df}{d\overline{R}^2} = \frac{\beta_p^2}{\overline{R}^4} + (1-\beta_p^2)\exp\left[2\alpha_1\beta_p^2\left(1/\sqrt{\overline{R}^2-\beta_p^2} - 1/\sqrt{1-\beta_p^2}\right)\right]\times$$

$$\alpha_1\beta_p^2\Big/\left(\overline{R}^2-\beta_p^2\right)^{3/2}\Big|_{\overline{R}=1} = \beta_p^2\left(\left(\sqrt{1-\beta_p^2}+\alpha_1\right)\Big/\sqrt{1-\beta_p^2}\right)$$

Substituting the derivative into (1a), and $f(\overline{R}^2)$ into (9), we write integral (8) as follows

$$\varphi = \sqrt{1+\alpha_1/\sqrt{1-\beta_p^2}}^{-1}\int_1^{\overline{R}}\left[\overline{R}\sqrt{\overline{R}^2-1}\right]^{-1}d\overline{R}$$

We get Eq (12) as a result of integration. Since the exact solution when $\beta_p = 0$ is represented by Eq (11), Eqs (11) and (12) were compared at different values of α_1. The comparison at the point $\overline{R} = 1.001$ showed agreement to the third decimal place.

In the limiting case, when $\beta_p = \beta_{pc}$, the first derivative approaches zero, $f'(1) \to 0$. Therefore to specify (12), it is necessary to obtain the second derivative. Upon differentiating the first derivative we get

$$d^2f/d(\overline{R}^2)^2 = -2\beta_p^2/\overline{R}_p^6 - \frac{(1-\beta_p^2)\alpha_1\beta_p^2\left(\alpha_1\beta_p^2+1.5\sqrt{\overline{R}^2-\beta_p^2}\right)}{(1-\beta_p^2)^3\exp\left[2\alpha_1\beta_p^2\left(1/\sqrt{1-\beta_p^2}-1/\sqrt{\overline{R}^2-\beta_p^2}\right)\right]} \quad (2a)$$

At the singular point $\beta_p = \beta_{pc}$ $\beta_p = \beta_{pc}$ when $\overline{R} = 1$, the second derivative will be $f''(1) = -\beta_{pc}^2(0.25+0.5\beta_{pc}^2)$ and is finite. Therefore in consideration of accuracy where $\overline{R}^2 = 1$, the third term in (1a) can be neglected and Eq (12) remains valid when $\beta_p = \beta_{pc}$ $\beta_p = \beta_{pc}$

2. Approximation at High Velocity

When $\beta_p = 1$, Eq (12) has a singularity. Therefore, to find increments of φ in the region $1 \le \overline{R} \le 1.001$ we shall employ a direct line equation which according to Eq. (11) will at $\alpha_1 = 0$ be $\overline{R} = 1/\cos\varphi$. Hence

$$\varphi = \arccos(1/\overline{R}) \quad (3a)$$

With $\overline{R}$=1.001 and $\varphi = 4.47\times10^{-2}$ (or $\varphi^0 = 2.56^\circ$), the polar angle for a particle moving near the speed of light changes from 2.56° with variation of $\overline{R}$ from 1 to 1.001.

3. Approximation for Apocenter

For ellipsoidal trajectories, numerical integration of Eq (8) was performed with small increments of velocity on the order of one part per thousand. It is necessary to estimate the impact this approximation has upon the polar angle of Eq (8). To this end, the relative radius $\overline{R}$ will be expressed through velocity $\upsilon_{r\min}$ determined from (10) and normalized to parameters at the pericenter. The relative radius will be substituted in the classical trajectory Eq (11). Hence we get

$$\Delta\varphi = \arccos\left(\sqrt{(\alpha_1+1)^2-\overline{\upsilon}_{r\min}^2}\Big/(\alpha_1+1)\right) \quad (4a)$$

In order to include the effect of relative velocity β_p we use Eq (12) to determine an asymptotic solution for the pericenter. It is easy to show that the apocenter asymptotic has an analogous effect. But, for that case, the parameters were referred to the transverse velocity at the apocenter υ_a and apocenter radius R_a, which depend on $\beta_a = \upsilon_a/c_1 = \beta_p/\overline{R}_a$ and $\alpha_{1a} = \alpha_1\overline{R}_a$. We introduce the influence factor k as a ratio of angle φ evaluated according to (12) to φ evaluated with $\beta_p = 0$. Hence we get

$$k = \sqrt{(1+\alpha_{1a})\Big/\left(1+\alpha_{1a}/\sqrt{1-\beta_a^2}\right)} \quad (5a)$$

Multiplying (4a) by (5a) yields an approximation for the apocenter as

$$\Delta\varphi \approx \sqrt{\frac{1+\alpha_1\overline{R}_a}{1+\alpha_1\overline{R}_a/\sqrt{1-\beta_p^2/\overline{R}_a^2}}}\arccos\left[\frac{\sqrt{(\alpha_1+1)^2-\overline{\upsilon}_r^2}}{\alpha_1+1}\right] \quad (6a)$$

Due to approximate nature of (6a) for limiting trajectories when $\beta_p \to \beta_{pc}$, numerical calculations with subsequent increase in υ have been done. In this case, the particle moves to the apocenter with the final angle φ.

References

[1] Xu Shaozhi and Xu Xiangqun, "A New Explanation of the "Mass-Velocity Relation"", Chinese Journal of Systems Engineering and Electronics, 5, (2) 68-71 (1994)

[2] T E Phipps, Jr., "Weber-type Laws of Action-at-a-Distance in Modern Physics," Apeiron, no 8, pp 8-14, 1990

[3] A K T Assis, "Weber's Law and Mass Variation", Physics Letters A 136, 277-280 (1989).

[4] J J Smulsky, **The Theory of Interactions**, (in Russian, Novosibirsk University Publishers, Novosibirsk, 1999)

[5] J J Smulsky, "Yes, Science is Confronted by a Great Revolution" Chinese Journal of Systems Engineering and Electronics 5 (2) 72-76 (1994)

[6] J J Smulsky, "The New Approach and Superluminal Particle Production," Physics Essays 7, (2) 153-166 (1994)

[7] T G Barnes, R R Pemper, and H L Armstrong, "A Classical Foundation for Electrodynamics," Creation Research Society Quarterly 14, 38-45 (1977)

[8] J J Smulsky, **The Electromagnetic and Gravitational Actions (The Non-relativistic Tractates)**, p 225 (in Russian, Novosibirsk Science Publishers, Novosibirsk, 1994)

[9] L D Landau, E M Lifshitz, **Field Theory** p 504 (Science Publishers, Moscow, 1973)

The New Fundamental Trajectories: Part 2 - Parabolic/Elliptic Trajectories

Joseph J. Smulsky
Institute of Earth's Cryosphere
Siberian Branch of Russian Academy of Sciences
P. O. Box 1230, Tyumen, 625000, RUSSIA; e-mails: smulski@ikz.ru, jsmulsky@mail.ru

This paper considers two-body interactions, which depend upon velocity and distance between the bodies. We use classical mechanics with constant mass and a force that depends on relative distance and velocity. The possible range of trajectories is studied: at small speeds the trajectories become classical, while at large speeds they become 'relativistic'. The results obtained provide mechanisms for trajectories at scales ranging from the micro-world to the macrocosm. Part 1 presented Sections 1-6 with Figures 1-3 and Eqs. (1-22), with hyperbola-like trajectories. Part 2 considers parabola-like trajectories, ellipse-like trajectories, and trajectories for repulsion interactions.

Key words: force, motion, trajectories, kinematics, momentum, pericenter, apocenter, attraction, repulsion, ellipse, parabola.

7. Introduction to Part 2

Our investigations [1, 2, 3] have shown that the force $\mathbf{F}$ of one point-charge q_1 acting on another charge q_2 moving with velocity $\mathbf{v}$ is determined by the relation

$$\mathbf{F} = \frac{q_1 q_2}{\varepsilon} \frac{\mathbf{R}(1-\beta^2)}{\left[R^2 - (\vec{\beta}\times\mathbf{R})^2\right]^{3/2}} \qquad (1)$$

where $\vec{\beta} = \mathbf{v}/c_1$, $c_1 = c/\sqrt{\varepsilon\mu}$; c is the speed of light in vacuum; ε and μ are the dielectric and magnetic permeability of the medium in which the charged objects are located.

With small charge velocity $\vec{\beta}$, the force (1) coincides with Coulomb's law. But as the velocity increases, the force decreases. And as the relative velocity between the charges approaches the velocity of electromagnetic action ($\beta \to 1$), the force tends to zero (except for $\vec{\beta}$ exactly perpendicular to $\mathbf{R}$). At this great speed, no action is exerted on such a body, and it is not accelerated.

According to (1) and Newton's second law of, the acceleration of one charge relative to another can be written as

$$\frac{d^2\mathbf{R}}{dt^2} = \mu_1 \frac{\mathbf{R}(1-\beta^2)}{\left[R^2 - (\vec{\beta}\times\mathbf{R})^2\right]^{3/2}} \qquad (2)$$

where μ_1 is the interaction constant; namely

$$\mu_1 = q_1 q_2 (m_1 + m_2)/\varepsilon m_1 m_2 \qquad (3)$$

By solving Eq. (2) we obtained in [2] a trajectory in a polar coordinate system as follows:

$$\varphi = \int d\overline{R}/\overline{R}^2\,\overline{\upsilon}_r \qquad (8)$$

$$\overline{\upsilon}_r = \frac{1}{\beta_p}\sqrt{1 - \frac{\beta_p^2}{\overline{R}^2} - \left(1-\beta_p^2\right)\exp\left[2\alpha_1\beta_p^2\left(\frac{1}{\sqrt{\overline{R}^2-\beta_p^2}} - \frac{1}{\sqrt{1-\beta_p^2}}\right)\right]} \qquad (9)$$

where $\overline{R} = R/R_p$ is the relative radius, R_p is the radius to the nearest point of the trajectory (pericenter), at which also $\upsilon_{R0} = 0$, $\overline{\upsilon}_r = \upsilon_r/\upsilon_p$ is the relative radial velocity, υ_p is the transverse velocity at the pericenter, $\beta_p = \upsilon_p/c_1$, $\alpha_1 = \mu_1/R_p\upsilon_p^2$ is the trajectory parameter.

In Part 1, Eqs. (8-9) at $\alpha_1 > -0.5$ were integrated numerically and found to produce hyperbola-like trajectories. Now the trajectories at $\alpha_1 \le -0.5$ will be studied.

8. Parabola-like and Ellipse-like Trajectories

Figure 4 shows sub-luminal trajectories with $\alpha_1 = -0.5$. In the classical case ($\beta_p \to 0$), the trajectory at $\alpha_1 = -0.5$ is parabolic. Here $\beta_p = \upsilon_p/c_1$, where υ_p is the transverse velocity of the particle at the pericenter. Even with $\beta_p = 0.1$, trajectory 1 is a highly-stretched ellipse. With an increase in speed β_p, the distance to apocenter $\overline{R}_a$ decreases and the angular distance to apocenter φ_a increases, and for the limiting trajectory 6 at $\beta_{pc} = 0.866$ it exceeds 2π. For this trajectory as well as for a limiting trajectory 7 in Fig. 1, the angle is counted from $\overline{R} = 1.001$. And in the region $1 < \overline{R} < 1.001$, $\varphi \to \infty$. In this case the particle is captured from the terminal region of space to a circular orbit. Trajectory 7 with $\beta_{t0} = 0.9$ and $\beta_{r0} = 0.2$, on which the particle speed tends to light speed at the pericenter, is also presented here (see Fig. 4). This hyperbolic trajectory with negative angle between asymptotes is similar to trajectory 6 in Fig. 3. (In these cases of hyperbola-like trajectories, the notation φ_a is the angle between asymptotes.)

Thus with an increase in the particle velocity, the parabolic trajectory transforms into an ellipse, in which the pericenter turns by an angle $\Delta\varphi$ per turn according to (21) The minimum distance to the apocenter $R_a = 5.456\ R_p$ is characteristic for a limiting trajectory With even higher speeds, the trajectories become hyperbolic, with light speed at the pericenter

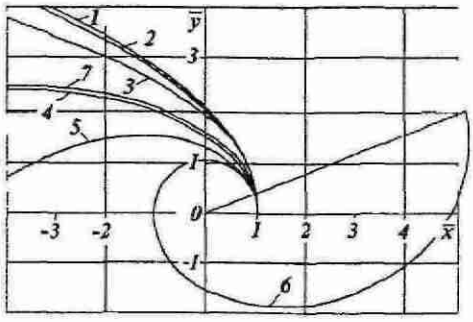

Figure 4 The trajectories at $\alpha_1 = -0.5$ and with sub-luminal speed at the pericenter ($\beta_p \le \beta_{pc}$) are trajectories 1-6

Table for Fig 4

№	1	2	3	4	5	6	7
β_p	0.1	0.3	0.5	0.7	0.8	0.866	1_0
α	-0.01	-0.09	-0.25	-0.49	-0.64	-0.75	-0.9
$\bar{R}_a / \beta_{r\infty}$	236411	2574	250.7	37.28	13.16	5.456	0.195*
φ_a^0	180.2	182.2	186.8	200.7	224.3	383.6'	-7.243

In the classical case ($\beta_p \to 0$), the trajectories at $0.5 > \alpha_1 > 1$ are ellipses Figure 5 shows the sub-luminal trajectories with $\alpha_1 = -0.7$ For $\beta_p \to 0$, the trajectory is an ellipse with radius of apocenter $R_a = 2.5R_p$ and the angular distance to apocenter is $\varphi_a = 180°$ As follows from Fig 5, at $\beta_p = 0.1$ the radius of apocenter decreases, and the angular distance to apocenter is $\varphi_a = 180.4°$ The eccentricity of elliptical trajectories decreases, and the turn of the apocenter increases with additional increase in velocity The apocenter of limiting trajectory 5 is slightly perturbed, therefore, trajectory 5 does not differ appreciably from a circular orbit. Trajectory 6, with light speed at the pericenter obtained at $\beta_{t0} = 0.8$ and $\beta_{R0} = 0.4$, is shown here The interaction parameter in this case ($-\alpha$) is $R_g / R_p = 1.12$, *i.e.*, it exceeds unity and radius of pericenter R_p is less than the gravitational radius R_g To determine the possible values of α, we make use of the Part 1 Eq (17) with parameter α_1 Then for limiting trajectories (15) we obtain the dependence of the interaction parameter $\alpha_c = \alpha$ with velocity at the pericenter β_{pc} of the form

$$\alpha_c = -2\beta_{pc}^2\sqrt{1-\beta_{pc}^2} \qquad (23)$$

It is easy to show that this expression has an extremum at $\beta_{pc} = \sqrt{2/3}$, and the highest value of the interaction parameter with respect to the modulus is $\alpha_c = -4/\sqrt{27}$ When $|\alpha| > |\alpha_c|$, so that $R_p < (\sqrt{27}/4)R_g$, trajectories will already have light speed at the pericenter, and these trajectories are either hyperbolic or terminal Thus, one can arrive at the following conclusions **1)** For an attracting center with radius less than gravitational radius R_g (the so- called 'black hole'), the particles can enter into the gravitational radius circle and do not fall on the attracting center **2)** Particles at the pericenter reach light speed, and due to a decrease in action on them go to infinity (or to the apocenter – for terminal trajectories) The only exception is a particle for which the velocity vector is directed exactly along the radius According to (5), with $h = 0$ and $R_0 \to \infty$ we obtain

$$\beta_r = \sqrt{1-(1-\beta_{r0}^2)\exp(-R_g/R)} \qquad (24)$$

In this case the particle will fall on the attracting center but its velocity, as it follows from (24), will be less than light speed

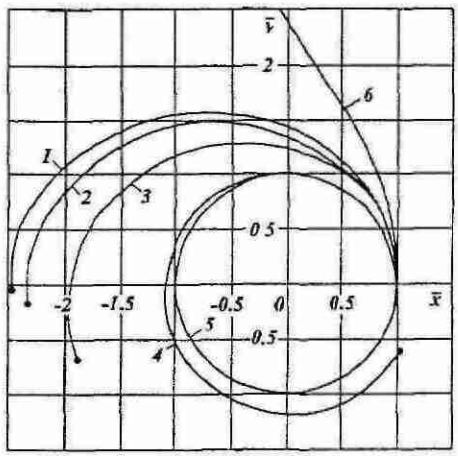

Figure 5. The trajectories at $\alpha_1 = -0.7$ and with sub-luminal speed at the pericenter ($\beta_p \le \beta_{pc}$) are trajectories 1-5

Table for Fig 5

№	1	2	3	4	5	6
β_p	0.1	0.3	0.5	0.7	0.714	1_0
α	-0.014	-0.126	-0.350	-0.686	-0.714	-1.12
$\bar{R}_a / \beta_{r\infty}$	2.482	2.334	1.991	1.220	1.031	0.331*
φ_a^0	180.4	184.5	197.5	328.1	1340'	40.26

In the classical case (10) for the particle moving radially from infinity, the speed is

$$\beta_r = \sqrt{\beta_{r0}^2 + R_g / R} \qquad (25)$$

If the particle was initially at rest ($\beta_{r0} = 0$) at infinity, upon reaching the radius $R = R_g$, its speed will be equal to light speed Since this movement is similar for both electromagnetic and gravitational interactions, the value R_g is best referred to as the *light radius*

Thus the results we derived indicate that for interactions propagating with velocity c_1, the attracting center at radius

$R \le R_g$ (a 'black hole') draws material more weakly than the classical attracting center – the action of which propagates instantaneously.

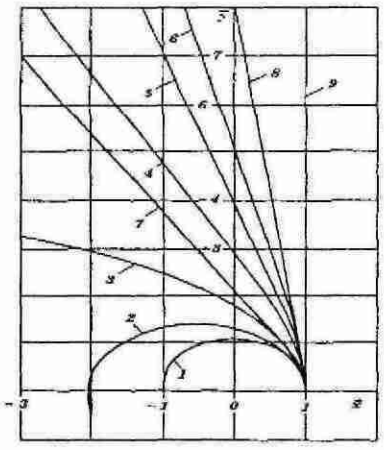

Figure 6. The trajectories with constant interaction parameter $\alpha = -0.3$.

Figure 6 presents trajectories at constant characteristics of interacting objects, *i.e.* those with constant parameter $\alpha = -0.3$. The eccentricity of the elliptical trajectories, numbered 1-3, increases with increasing speed at the pericenter β_p. Then the trajectories diverge and pass into the hyperbolic trajectories, numbered 4-6, where the angle between asymptotes φ_a grows with increasing β_p. At larger speed at infinity $\beta_{p\infty}$ (trajectory 8), light speed is attained at the pericenter, and the angle φ_a increases and tends to $\pi/2$ for light-speed trajectory 9. We note that at $\beta_p = \beta_{pc}$ (trajectory 7), the angle between asymptotes is small because the integration was accomplished to $\overline{R} = 1.001$.

For Fig. 7, the trajectories of two-body interactions depend upon parameters α_1 and β_p as follows: curve 1 – Eq. (15); curve 2 – Eq. (22) at $\beta_p = \beta_{tp} = \beta_{0p}$; Classes of trajectories: G – hyperbola-like; P – parabola-like; E – ellipse-like; C – finite trajectories which result in a circle; S – trajectories with light speed at the pericenter; N – absence of trajectories.

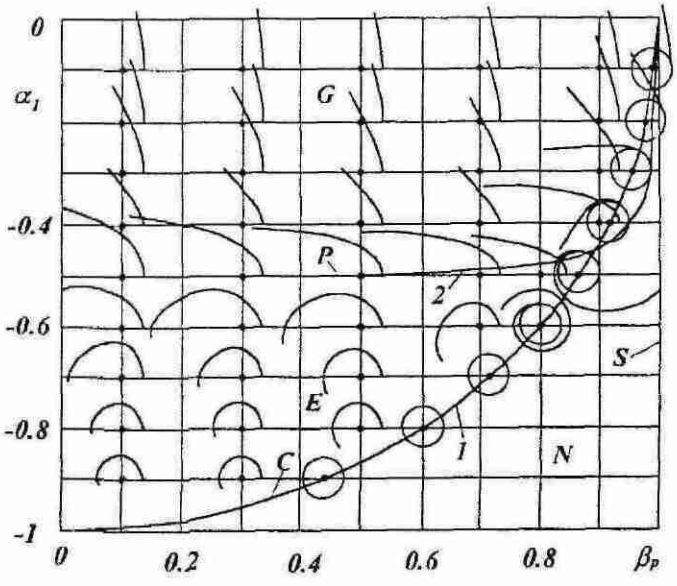

Figure 7. The panorama of trajectories of two-body interactions depending on parameters α_1 and β_p.

Table for Figure 6. Trajectories with constant interaction parameter $\alpha = -0.3$.

№	1	2	3	4	5	6	7	8	9
β_p	0.408	0.463	0.548	0.707	0.866	0.913	0.988	1_{-0}	1
α_1	−0.9	−0.7	−0.5	−0.3	−0.2	−0.18	−0.154	−0.151	−0.15
$\overline{R}_a / \beta_{p\infty}$ *	1.036	2.074	157	0.488*	0.739*	0.809*	0.913*	0.968*	1.0*
φ_∞^0	189.9	193.5	189.1	62.56	73.78	77.56	59.40!	82.72	90

Variation of trajectories for different α_1 and β_p is shown in Fig. 7. Curve 1 from Eq. (15) limits from below, and on the right the area of existences of trajectories with body velocity in the pericenter less than light velocity. This curve gives multiple trajectories α_{1c}, which are transient into circular orbit, *i.e.* on these trajectories the particle is captured on a circular orbit.

Curve 2, representing Eq. (22), detaches the hyperbola-like trajectories from ellipse-like trajectories. Curves 1 and 2 intersect at the point $\alpha_1 = -0.450764$ and $\beta_p = 0.89264$. The points of curve 2 at $0 < \beta_p \le 0.89264$ give the parabolic trajectories on which the particle has zero velocity at infinity.

9. The Trajectories of Repulsion and Full Period of the Trajectories

Figure 8 presents the hyperbolic trajectories when the interacting bodies are repulsed. Calculations were performed at three values of α_1 (0.3, 0.5, 1.5) and variations of β_p. With an increase in β_p, the half-angle between asymptotes φ_a increases and tends to $\pi/2$ for the light speed trajectory. The interaction parameter α_1 is positive for the repulsion trajectories and can be more than unity. The particle velocity increases when it moves away from the center.

Some full-period trajectories are shown in Fig 9 Previously (Fig 3), we studied half-periods of these trajectories Cyclical trajectories 1 and 4 are open curves Trajectory 1 (with jumps) has three periods per turn, and trajectory 4 has three and one-half turns per period Trajectory 6 traverses itself at a great distance from the attracting center One sees that an error is possible if one uses Coulomb's law for calculating parameters of attracting centers while measuring trajectory characteristics For example (see trajectory 6), one can define a greater diameter of attracting center than actually exists, or an actual interaction of attraction could be wrongly defined as an interaction of repulsion

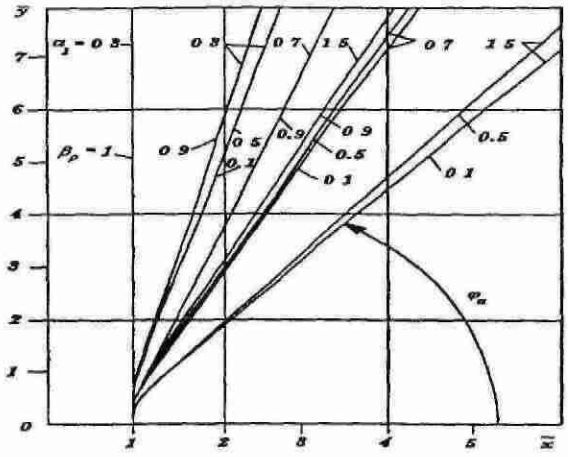

Figure 8 Trajectories of Repulsion

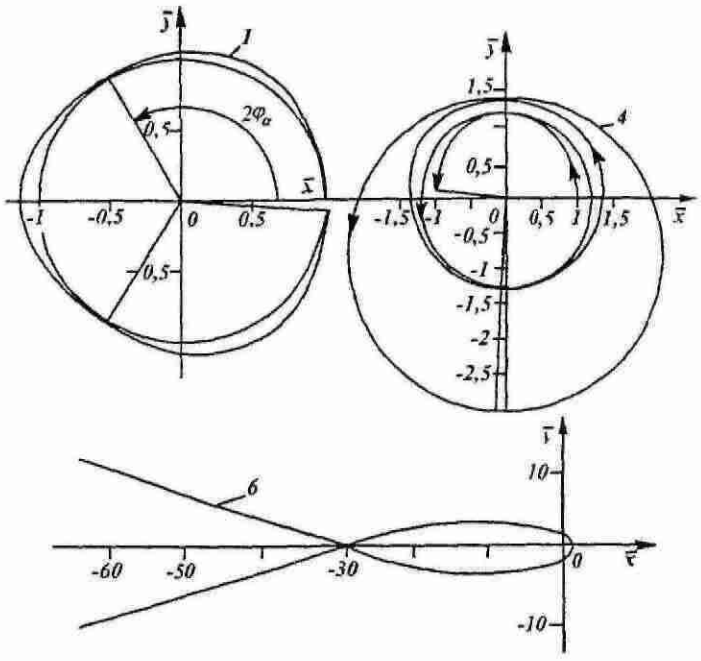

Figure 9 Trajectories for full period at light velocity in the pericenter Numbers of trajectories are in accordance with Fig 3

Table for Fig 8 Trajectories of Repulsion.

α_1	0 3	0 3	0 3	0 3	0 7	0 7	0 7	1 5	1 5	1 5
β_P	0 1	0 5	0 9	1 0	0 1	0 5	0 9	0 1	0 5	0 9
α	006	0 15	0 486	0 6	0 014	0 35	1 134	0 03	0 75	2 43
$\beta_{r\infty}$	0 126	0 61	0 968	1 0	0 1543	0 707	0 993	0 198	0 827	0 9999
φ_a^o	76 7	76 9	79 1	90	65 7	66 6	73 2	53 2	55 6	69 0

The results we obtained should be compared and carefully analyzed to comprehend their significance One may then see that they can provide new mechanisms for understanding natural phenomena. For example, based on the kinematics parameters of a charged particle, the trajectories may describe existing steady-state orbits of electrons in an atom, or the transition of an electron from one orbit to another, or the capture of a particle into a nucleus or an atomic shell

If one applies these results to gravitation, it is seen that many phenomena have the exact opposite effect of that predicted by General Relativity Theory For example, if gravitational effects propagate at light speed, black holes' should not exist If astronomers discovered this, they would likely conclude that gravity propagates with infinite speed – or at least a speed much greater than the speed of light in vacuum

10. Conclusions

- The new force expression describes the electromagnetic interactions of two bodies with small and high relative velocities
- Small particles of the microworld, and large bodies of the macrocosm (if the propagation of gravitational interaction is equal to c_1), are moving on the predicted trajectories
- For most of the twentieth century, the analysis of experiments on the interaction and scattering of charged particles has been based on classical trajectories Different kinds of elementary particles and their properties have been defined by the use of trajectories based on Coulomb's law However, trajectories of particles are better described by another law, so many conclusions of modern physics for a host of elementary particles are suspect
- A new analysis of particle physics, based on real trajectories, is needed to draw correct conclusions from existing experimental data We will discover the real world only if particle experiments (beginning with Rutherford's experiments) are re analyzed with assistance of the new fundamental trajectories

Acknowledgement

David L Bergman volunteered to help with the editing necessary for publishing my paper in English I am most grateful for

his assistance The Editor Cynthia K Whitney raised the technical point discussed in Related Correspondence below

References

[1] J J Smulsky "The New Approach and Superluminal Particle Production', Physics Essays 7, (2) 153-166 (1994)

[2] J J Smulsky The Theory of Interactions (In Russian), Novosibirsk University Publishers, 294 pages, 1999

[3] J J Smulsky, The New Fundamental Trajectories Part 1 Hyperbolic Trajectories' Galilean Electrodynamics

Related Correspondence

Comment from the Editor to the Author:

You said Eq (1) makes $\mathbf{F} \to 0$ when $\beta \to 1$ This is certainly true if $\bar{\beta}$ is not perpendicular to $\mathbf{R}$ But if they are perpendicular, then the right hand side of Eq (1) becomes '0/0' Approaching the limit, you have $(1-\beta^2)/(1-\beta^2)^{3/2}$ Perhaps this approaches infinity rather than zero What do you think, and how does it affect your presentation?

Reply from the Author:

In 1968 I derived the force law (1) as a result of solving Maxwell's equations Until 1994 I doubted the infinity of force when $\beta \to 1$ and $\bar{\beta}$ is perpendicular to $\mathbf{R}$, and I made a lot of different investigations When I had calculated the force with which charged bodies of different forms act on a moving charged particle, and when I had calculated interaction of two charged particles in different possible cases, I was convinced that infinite force when $\bar{\beta}$ is perpendicular to $\mathbf{R}$ is not a mistake

If the charged body acts on a moving charged particle, the distance $\mathbf{R}$ is perpendicular to $\bar{\beta}$ for a finite number of body points Therefore, the aggregate force of such a body will certainly always be non infinite If two charged point particles move under their interaction, there is only one point on their trajectories where $\bar{\beta}$ is perpendicular to $\mathbf{R}$ At this one point, for $\beta \to 1$ the force tends to infinity But the charged particle moves across the point in an infinitesimally small time Therefore the infinite force and infinite acceleration do not give infinite change of velocity or distance

Correspondence

Orbits Do Not Have Pimples (continued from page 46)

References

[1] Shapiro *et al* "Mercury's Perihelion Advance Determination by Radar," Physical Review Letters 28 1594-7 (1971)

[2] Reasenberg *et al* "Viking Relativity Experiment Verification of Signal Retardation by Solar Gravity", *Astrophysical Journal Letters* 219-21 (1979)

[3] Hayden "Light Speed as a Function of Gravitational Potential", Galilean Electrodynamics 1 (2) 15-17 (1990)

[4] Whitney "Bending, Stretching, Shrinking—of Light," *Galilean Electrodynamics* 11 (1) 2,9,10,15 (2000)

Ronald R. Hatch
1142 Lakme Avenue
Wilmington, CA 90744

C.K.W. Again

Even with no orbit pimples allowed, I fear there are still estimation risks to worry about. Estimating gravitational delay requires estimating baseline delay, which requires an orbit model Whether Newtonian or Einsteinian, the orbit model is certainly pimple-free, but it also involves parameters (in particular, positions of everything at relevant times) that are estimated from optical data. Optical data is subject to gravitational bending When the gravitational delay on a signal from Venus is large, the gravitational displacement on the angular position of Venus is similarly large This makes for a potential error on the estimated light-ray grazing-range-to-Sun, and hence an error on the light-ray Venus-to-Earth range, and hence the baseline delay. Is *this* potential error source consistently accounted for? Who knows, it just isn't mentioned

Cynthia K. Whitney, Editor

Newton's Too-Special Law of Gravitation

Our experience of gravitation is limited to spherical bodies in almost circular orbits, often at very great distances Gravitation creates spherical bodies, and the spherical form is also demanded by Newton's law, which describes gravity by approximating masses as points But this convenient approximation does not reveal much about the mechanism behind gravitation, which therefore hides its secrets behind spherical symmetry and mathematical simplicity

Newton's Law

Since Newton's law is valid only for spherical bodies, it is of interest to discuss mathematical descriptions that are valid for *aspherical* bodies. By considering ideas presented in [1], we find that it is also of interest to discuss gravitation for *very* massive bodies A third possible completion to Newton's law is a *finite* speed for the propagation of gravity

The following discussions are based on an assumption of absolute space and time — independent of each other

Aspherical Bodies

Thought experiments can help us to find descriptions for the aspherical case One method is to consider two spherical bodies to constitute one aspherical body The attraction between these bodies also demonstrates gravitation's tendency to create one sphere out of two Another way is to consider an aspherical body to consist of an infinite number of infinitesimal parts, whereby their form does not matter Newton's law must be valid *all* the time when the body is put into many parts

The demands mentioned above can be fulfilled only if summation over a finite number of bodies is replaced by integration over a large volume, where each volume element has a defined